A Reanalysis of the Spectra Observed in JONSWAP

J. A. BATTJES, T. J. ZITMAN AND L. H. HOLTHUIJSEN

Dept. of Civil Engineering, Delft University of Technology, Delft, The Netherlands

(Manuscript received 28 July 1986, in final form 4 March 1987)

ABSTRACT

The frequency spectra of wind-driven waves observed during JONSWAP are reanalyzed to establish whether the Toba formulation for the high-frequency tail ($\sim f^{-4}$) fits the data better than the Phillips formulation ($\sim f^{-5}$) used originally in the JONSWAP project. The results indicate that the f^{-4} tail provides a statistically better fit to the observed spectra. The proportionality factor in Toba's spectrum, which is theoretically expected to be a universal constant, is found to be uncorrelated with the growth stage of the waves. There is a relatively large scatter in the observed values, which can partly be ascribed to the influence of tidal currents.

1. Introduction

The energy spectrum of wind waves at sea has been studied extensively for the purpose of understanding and modeling its evolution in a variety of geophysical conditions. In so-called ideal conditions of wave generation (a steady, uniform windfield at right angles to a straight upwind coastline), the spectral distribution of wave energy over the frequencies appears to have a standard shape, regardless of the values of its scale parameters, which are controlled by external conditions (see e.g. Hasselmann et al., 1973).

The tendency towards a standard spectral shape can manifest itself also in non-ideal conditions of wave generation (Hasselmann et al., 1976), provided the changes in the controlling external parameters (in particular the wind velocity) are sufficiently slow compared to the time scale of the spectral evolution. This gives added weight to knowledge about the standard spectral shape in ideal conditions. In a pioneering paper, Phillips (1958) argued that there should be a range of frequencies where the spectral density $E(f)$ is saturated at a level determined exclusively by the local frequency (f) and the gravitational acceleration (g). On dimensional grounds this saturation level should be proportional to $g^2 f^{-5}$. It can be written as

$$E(f) = (2\pi)^{-4} \alpha g^2 f^{-5} \tag{1}$$

with α a universal constant. The Phillips formulation for the equilibrium range was applied by Pierson and Moskowitz (1964) for the spectrum of fully developed seas, and by Hasselmann et al. (1973) for the spectrum of growing seas (the JONSWAP spectrum). However, in the latter study, it turned out that α varied with the growth stage instead of being a constant, as had been inferred by Phillips.

Another approach to the formulation of the saturation range is due to Toba (1972, 1973). It is based on his so-called three seconds power law for the significant wave height (H_s) and the significant period (T_s). Stated in spectral terms, this law implies that the integral of the spectral densities, or the variance of the surface elevation (ϵ) and the peak frequency (f_m) are related according to

$$\epsilon \sim g u_* f_m^{-3} \tag{2}$$

where u_* is the shear velocity of the wind over the water surface. The saturation spectral density which Toba (1973) deduced from this on similarity grounds can be written as

$$E(f) = (2\pi)^{-3} \beta g u_* f^{-4} \tag{3}$$

with β a universal constant. Initially, empirical support for Toba's formulation (3) was obtained in laboratory experiments (Toba, 1973), and somewhat later in field observations (Kawai et al., 1977).

Toba's formulation (3) and the JONSWAP spectrum were published in the same year (1973). The JONSWAP work received almost instant recognition, and quickly became well known in the international literature. This was not the case—undeservedly, in our opinion—for Toba's work. This has begun to change only recently, with the presentation of further empirical evidence supporting (3) by Mitsuyasu et al. (1980), Kahma (1981), Forristall (1981), and Donelan et al. (1985), and with theoretical work of Kitaigorodskii (1983) and Phillips (1985). In the latter publication, Phillips in fact abandons his original, simple dimensional arguments leading to (1), in favor of a detailed analysis of the source terms in the spectral action balance, leading to (3) as well as to many other results. In the remainder of this paper we shall nevertheless refer to (1) and (3) as being due to Phillips and Toba, these being the respective pioneer authors of these models.

It was decided to reanalyze the original JONSWAP dataset with the purpose of investigating the fit of

Toba's formulation to those data. The JONSWAP data were chosen because they are considered to represent virtually ideal generation conditions, and because the JONSWAP spectrum has widely been accepted in the oceanographic and engineering communities. Moreover, the dataset is well documented.

In the following, brief comments are made regarding the JONSWAP data used in the present study. This is followed by a description of models which were used for the high-frequency range and for the entire spectrum separately. The procedures of fitting these models to the data and of establishing quantitative measures for goodness-of-fit are described next; this includes a discussion of the influence of an ambient current on the observed spectra. The best-fit spectral parameters are considered as a function of the dimensionless peak frequency which serves as a growth stage parameter. Finally, the results are presented and discussed.

2. JONSWAP data

The spectra analyzed in this study were obtained in the Joint North Sea Wave Project (JONSWAP, see Hasselmann et al., 1973). They were kindly made available to the present authors for the purpose of a reanalysis. We refer to Hasselmann et al. (1973) and Müller (1976) for a description of the methods of observation and analysis and the geophysical conditions during these observations.

The available spectra were selected in JONSWAP to represent so-called ideal generation cases, in which case a homogeneous, stationary wind blows over deep water orthogonally from a long and straight coastline. A total of 108 of such spectra from the 1969 campaign of JONSWAP was available. This represents 89% of the original spectra used by Hasselmann et al. (1973); the remaining 11% are the 13 spectra of the 1968 JONSWAP campaign. Of the 108 spectra, 9 were deemed to be double-peaked. These were removed so that ultimately 99 of the 121 original spectra used in JONSWAP were reanalyzed. The key parameters of these spectra are given in appendix A.

The spectra were reanalyzed to see whether the saturation level suggested by Toba (1973) fits the observations better than that suggested by Phillips (1958), and to estimate the corresponding model parameters. Since the Toba formulation contains the friction wind velocity u_*, the value of the wind speed at 10 m elevation U_{10}, in the JONSWAP dataset has been transformed to the value of u_*. We have used Garrett's (1977) formulation:

$$U_z = (u_*/\kappa)\ln(z/z_0)$$
$$z_0 = 0.0144\,u_*^2/g \qquad (4)$$

where κ is the von Karman constant ($\kappa = 0.4$ was used) and $z = 10$ m.

3. The spectral models

The spectral models to be fitted to the JONSWAP data for purpose of comparison are those given by Phillips (1958) and Toba (1973), Eqs. (1) and (3). These are nominally valid for a high-frequency range only. A comparison of their relative merits should therefore be based on an analysis restricted to that high-frequency range. The conclusions from such an analysis form the principal results of the present paper.

From a practical point of view, it is also of interest to know the significance of a possible difference of goodness-of-fit in the high-frequency range, relative to the quality of present-day formulations of the remaining parts of the spectrum, viz. the peak and the low-frequency flank. For this reason an additional analysis has been performed in the full frequency range, assuming either the f^{-4} tail or the f^{-5} tail, each supplemented with a JONSWAP-type peak and low-frequency flank, as described by the equations

$$E(f) = (2\pi)^{-4}\alpha g^2 f^{-5}\exp\left[-\frac{5}{4}\left(\frac{f}{f_m}\right)^{-4}\right]\Gamma(f) \qquad (5)$$

and

$$E(f) = (2\pi)^{-3}\beta g u_* f^{-4}\exp\left[-\left(\frac{f}{f_m}\right)^{-4}\right]\Gamma(f) \qquad (6)$$

in which $\Gamma(f)$ is the JONSWAP-type peak enhancement function:

$$\Gamma(f) = \gamma^{\exp[-(1-f/f_m)^2/2\sigma^2]}$$

$$\sigma = \sigma_a \quad \text{for} \quad f \leqslant f_m, \quad \sigma = \sigma_b \quad \text{for} \quad f > f_m. \qquad (7)$$

(The factor $5/4$ which appears in the exponential function in (5) should not be included in (6), because f_m is defined as the frequency of the spectral peak.)

The spectral forms given above are nominally valid in a reference frame moving with the mean current (if that is present). The observed spectra are obtained from measurements at fixed points, and may therefore be affected by Doppler shifts due to a mean current. The relevance of this for the present data is discussed below.

4. Analysis procedure

a. Frequency ranges

In the following, the lower and upper limits of the frequency ranges considered (high-frequency or full-frequency range) are denoted by f_1 and f_2.

The spectra observed in JONSWAP are given at frequencies between $f_{\min} = 1/128$ Hz and $f_{\max} = 127/128$ Hz, with a sample interval of $1/128$ Hz. For the high-frequency range analysis, the lower and upper cutoff frequencies, f_1 and f_2, were chosen as $f_1 = 1.5f_m$ and $f_2 = f_{\max}$. For the full-frequency range analysis, f_1 was chosen as $f_1 = 0.8f_m$, to avoid contamination with low-frequency swell that may have been present in the ob-

servations (see Müller, 1976), and the value of f_2 was taken as either $2f_m$ or f_{max} (the lowest of these two).

For each observed spectrum, the value of f_m needed to determine f_1 and f_2 was taken from Müller (1976) (only for this purpose). Spectra for which the interval (f_1, f_2) contained less than 30 independent spectral estimates were ignored in the analysis for reasons explained in section 4d. This occurred for 17 spectra in the high-frequency range analysis (see appendix A). In the full-frequency range analysis all of the 99 spectra were accepted.

b. *Influence of current velocity*

The JONSWAP measurements were carried out at fixed points in the presence of tidal currents. This causes an observed spectrum $E_o(f_o)$ to differ from the prevailing wave spectrum as would be observed in a frame of reference moving with the current, the so-called intrinsic spectrum $E_i(f_i)$, due to the Doppler shift between f_o and f_i.

Ideally, one should estimate $E_i(f_i)$. This requires knowledge not only of $E_o(f_o)$ but also of the directional spreading of the wave energy per frequency, and of the current velocity U for each spectrum. Neither of these was available to us. The analyses presented below have therefore been performed on $E_o(f_o)$.

A quantitative assessment of the errors introduced by using the spectra without correction for current influence can be made using standard formulations for spectral transformations in case of moving reference systems (see e.g. Kitaigorodskii et al., 1975). This has been done for the high-frequency range from 0.5 Hz to 1.0 Hz only, assuming unidirectional waves and a following current or an opposing current with a velocity of 0.3 m s^{-1}, midway in the range of the observed velocities (0.2 to 0.4 m s^{-1}) reported by Hasselmann et al. (1973). The results can be summarized as follows.

The calculated ratio of the observed spectral density to the intrinsic density, averaged over the frequencies from 0.5 Hz to 1.0 Hz, is about 0.8 in case of a following current and about 1.4 in case of an opposing current. The estimated values of α and β would be affected in the same proportion in a random manner, assuming independence between the time of the wave measurements and the phase of the tidal cycle. The current would therefore introduce a random variation with a factor of nearly two in the estimated values of α and β, with a positive bias of about 10%.

Since the current influence of the frequency shift and on the spectral density increases with frequency, the slope of the high frequency tail of the spectrum is affected too. For an intrinsic spectrum with an f^n tail with $n = -5$ or $n = -4$, the average value of n for the observed spectrum in the range from 0.5 to 1.0 Hz has been calculated. It is found to deviate less than 10% in absolute value from the n-value for the intrinsic spectrum. The scatter associated with this does not therefore invalidate the use of the uncorrected data to discriminate between a -5 an f^{-5} and f^{-4} tail.

The conclusion from the above is that the distortion of the observed spectra due to Doppler shifting causes a considerable variation and a slight bias in the estimated values of α and β, without impairing the possibility of discriminating between the two spectral models considered.

c. *Parameter estimation*

For the high-frequency range analysis, the values of α and β were estimated simply as the average level of $(2\pi)^4 g^{-2} f^5 E(f)$ and $(2\pi)^3 (g u_*)^{-1} f^4 E(f)$ respectively, between the frequencies f_1 and f_2.

For the full-frequency range analysis, the above model spectra $[E(f)]$ are fitted to the observed spectra $[E'(f)]$ with a nonlinear least-squares method which minimizes the integrated squared error V, defined as

$$V = \int_{f_1}^{f_2} [E'(f) - E(f)]^2 df \tag{8}$$

with the side condition that the total energy for each spectrum is conserved. The minimization procedure used in this method is the simplex method described by Nelder and Mead (1965), which is essentially an efficient gradient method. In the fit procedure used here, the spectral parameters are estimated simultaneously, based on an overall measure of fit. We prefer this over the method used by Müller (1976) in which the parameters are estimated successively, based on a fit to various parts of the spectrum separately. However, for the model spectrum described by Eqs. (5) and (7) (i.e. the original JONSWAP model) the method provides parameter estimates that are close to those of Müller (1976).

The best-fit parameter values obtained for each observed spectrum are considered as a function of growth stage, for which the dimensionless peak frequency ν was chosen:

$$\nu = U_{10} f_m / g. \tag{9}$$

A linear least-squares method for log scales was used to determine the coefficient r and exponent s of the assumed power-law relationships between the spectral parameter considered (a_k, say) and ν:

$$a_k = r_k \nu^{s_k}. \tag{10}$$

d. *Goodness-of-fit*

To establish quantitatively which of the two models (the f^{-4} or the f^{-5} tail) fits the JONSWAP observations best, the minimized values of the squared deviation V were used. However, this value is influenced by both the energy and frequency scales of the spectrum, which are irrelevant for a shape analysis. Therefore, a normalized squared deviation ($\hat{V}$) is considered:

$$\hat{V} = V f_m / \epsilon^2 \tag{11}$$

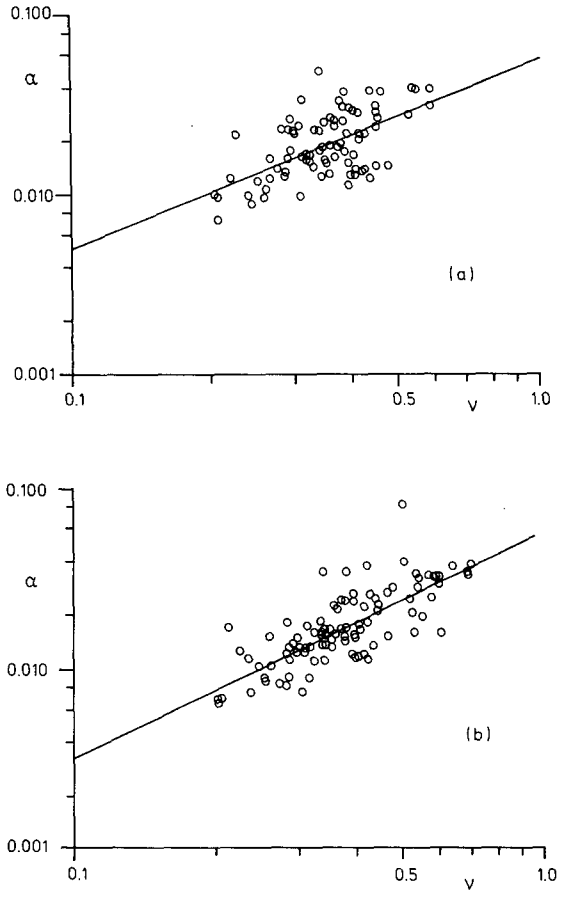

FIG. 1. Data points: best-fit values of Phillips' α vs dimensionless peak frequency ν. The straight line represents the best-fit power law relationship (10). (a) high-frequency range analysis; (b) full-frequency range analysis.

where ϵ is the total energy in the frequency range being analyzed:

$$\epsilon = \int_{f_1}^{f_2} E(f)df. \tag{12}$$

In order to compare the fit of two models to the data, the difference between the respective normalized minimum squared deviations is considered, written as Q:

$$Q = \hat{V}_P - \hat{V}_T. \tag{13}$$

The subscripts P and T refer to the spectral models with a high-frequency tail according to Phillips and Toba, respectively.

The values of Q should be nearly Gaussian-distributed if the number of observed spectral density estimates (which are each χ^2-distributed) in the integral of (8) is sufficiently large. For this reason a minimum of 30 frequency bands was chosen. A Student's t-test was used to test the hypothesis that the expected value of Q is positive or negative or equal to zero at a given level of confidence. If e.g., Q is found to be significantly larger than zero ($\hat{V}_P > \hat{V}_T$ on the average), then the Toba model (with the f^{-4} tail) is said to provide a statistically significant better fit to the observed spectra than the Phillips model (with the f^{-5} tail) at that level of confidence.

5. Results

a. *Spectral parameters*

The mean and standard deviation of the estimated values of α and β and the spectral shape parameters of the best-fit spectra are given in Table 1, together with the coefficients and exponents of the power law dependencies on the dimensionless peak frequency ν [Eq. (10)]. The value of the peak frequency in this analysis was taken from the full-frequency range analysis using either Phillips's model or Toba's model as appropriate for the respective model parameters. A graphical impression of the variation of the scale parameters α and β with ν is given in Figs. 1 and 2.

b. *Goodness-of-fit*

The joint variations of the normalized error measures $\hat{V}_P$ and $\hat{V}_T$ for the two frequency ranges are given

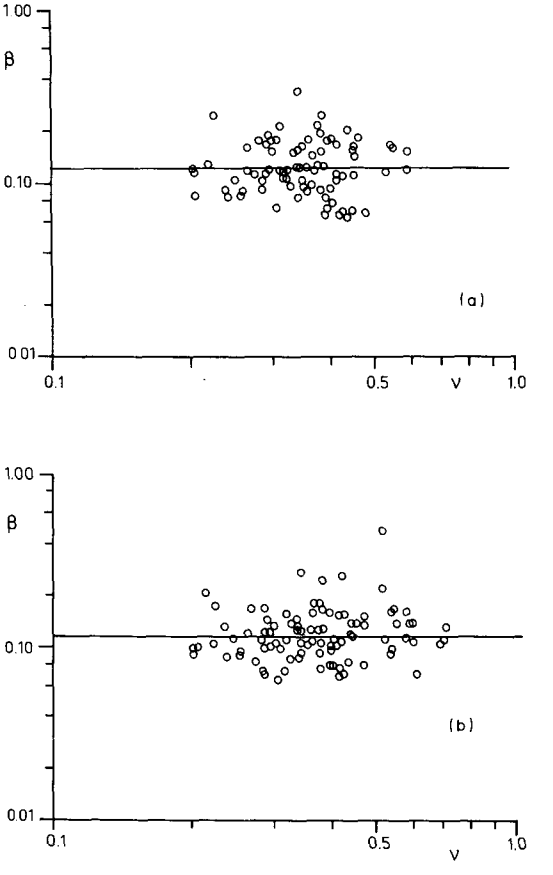

FIG. 2. As in Fig. 1 except for best-fit values of Toba's β vs dimensionless peak frequency ν.

TABLE 1. Mean and standard deviation of the spectral parameters, and coefficients and exponents of the power law (10).

	a_k	Mean	Standard deviation	r_k	s_k
		High-frequency range analysis			
Phillips	α	0.020	0.009	0.056	1.06
Toba	β	0.129	0.062	0.126	0.23
		Full-frequency range analysis			
Phillips	α	0.019	0.010	0.056	1.24
	γ	3.07	0.85	2.57	−0.15
	σ_a	0.10	0.11	0.08	−0.15
	σ_b	0.061	0.05	0.12	0.12
Toba	β	0.127	0.055	0.119	0.01
	γ	3.64	1.08	3.02	−0.16
	σ_a	0.12	0.13	0.07	−0.28
	σ_b	0.17	0.05	0.14	0.18

in Fig. 3, and the histograms of their difference Q are shown in Fig. 4.

For the high-frequency range analysis, the mean and standard deviation of Q are 0.0948 and 0.0519 respectively, based on 82 observed spectra. With the t-test the hypothesis that the expected value of Q is larger than zero is accepted even at a confidence level as high as 99.9%.

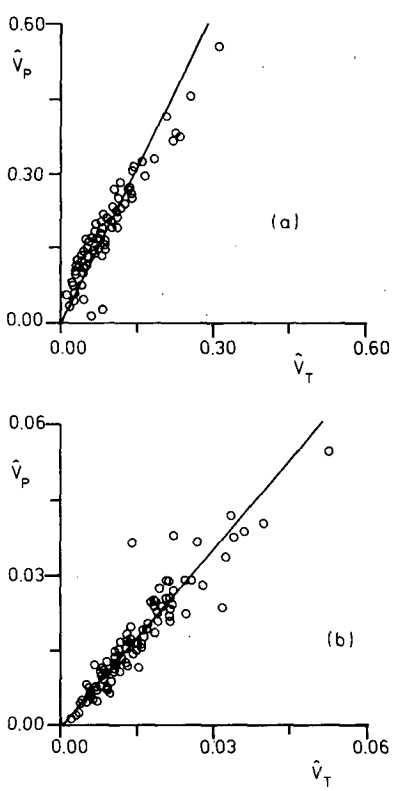

FIG. 3. Data points: normalized error of measurements $\hat{V}_P$ (Phillips) and $\hat{V}_T$ (Toba) per observed spectrum. The straight line represents the best-fit proportional relationship. (a) high-frequency range analysis; (b) full-frequency range analysis.

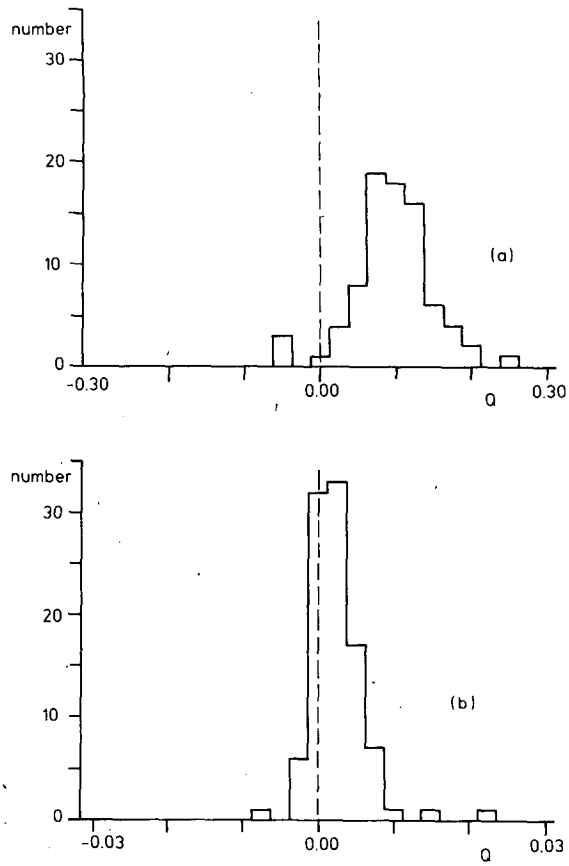

FIG. 4. Histograms of Q. (a) high-frequency range analysis; (b) full-frequency range analysis.

For the full-frequency range analysis, based on 99 spectra, the mean and standard deviation of Q are 0.00320 and 0.00782 respectively. Again the hypothesis that Q is positive is accepted with the t-test at a confidence level of 99.9%.

6. Discussion

a. Relative goodness-of-fit

The principal result of the present study consists of the calculated joint variation of the error measures $\hat{V}_P$ and $\hat{V}_T$, and their differences Q, based on the high-frequency range analysis (Figs. 3a and 4a). These clearly show that the f^{-4} tail fits the observed spectra significantly better than the f^{-5} tail. The difference in fit is statistically significant, based on the t-test, as indicated in section 5b.

The above quantitative assessment of the goodness-of-fit of an f^{-4} or an f^{-5} tail cannot be compared with similar quantitative tests in the literature since such tests have not been carried out before, at least not to the knowledge of the present authors. Instead, several

investigators have used a more graphic approach in which the observed spectra were multiplied by f^4 or f^5. The functions thus obtained appeared to be more nearly a constant as a function of frequency with the f^4 multiplication than with the f^5 multiplication (e.g., Donelan et al., 1985; Forristall, 1981; Kahma, 1981; Mitsuyasu et al., 1980; Toba, 1973).

As noted above, a full-frequency range analysis has been carried out in order to investigate how important a possible improvement in the formulation of the high-frequency tail is in relation to the natural variability and the imperfectness in present-day modeling of the spectral peak and the low-frequency range. The results in terms of $\hat{V}_P$, $\hat{V}_T$ and $Q = \hat{V}_P - \hat{V}_T$ are given in Figs. 3b and 4b. Inspection of these figures shows that for the entire spectrum the spectral model (6), with the Toba formulation for the equilibrium range, on the average is marginally better than the model (5) with the Phillips formulation for the equilibrium range.

b. *Spectral parameters*

The present discussion of the spectral parameters will focus on the energy scale parameter β and its possible variation with the dimensionless peak frequency ν, compared to the parameter α.

The best-fit values of β have been plotted against ν in Fig. 2, together with the calculated best-fitting power law relationship between the two. No trend of β with ν is visible. In fact, the hypothesis that the exponent (s) in the power law relationship between β and ν is zero is accepted at a 99.9% confidence level, using a t-test (Draper and Smith, 1981). This observed lack of systematic variation of Toba's β with the growth stage parameter ν contrast with the variation of Phillips' α (see Fig. 1). It supports Toba's original model, insofar as this predicted that β should be a constant. However,

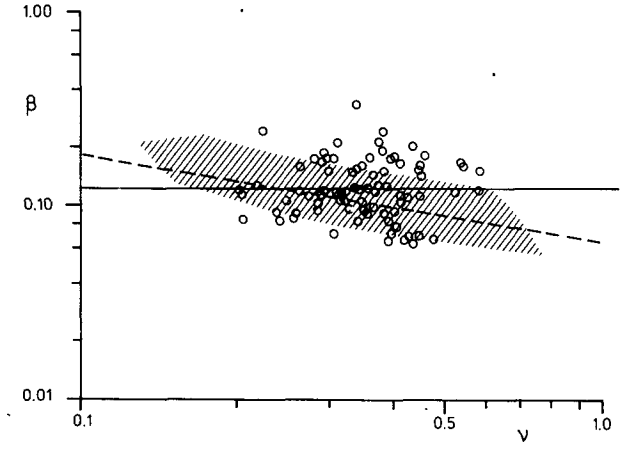

FIG. 5. Data points and drawn line: see Fig. 2a. The hatched area and the dashed line represent the range of the results of Donelan et al. (1985) and the corresponding best-fit power law relationship (B5) (see appendix B).

TABLE 2. Mean value of the energy scale parameter β from various sources.

Author	Mean value of β
Laboratory	
Toba (1973)	0.02
Field	
Kondo et al. (1973)	0.06
Kawai et al. (1977)	0.062
Mitsuyasu et al. (1980)	0.087
Kahma (1981)	0.11
Forristall (1981)	0.11
Donelan et al. (1985)	0.11
This study (JONSWAP)	0.13

the large scatter in the observed values exceeds the range to be expected on account of the influence of tidal currents. (The unexplained scatter did not decrease by correlating β with ν_*, the peak frequency scaled with g/u_*.)

Among the previously published numerical results concerning Toba's β, only those presented by Donelan et al. (1985) indicate a clear trend with ν (see appendix B). A comparison of these results with those obtained in this paper is given in Fig. 5. It is clear that the β-values found by Donelan et al. are correlated with ν, in contrast with those obtained in the present study from the JONSWAP data. This suggests that the conditions during the observations of Donelan et al. were more homogeneous (with less unknown variability in geophysical factors) than those during JONSWAP. This may well be due to the fact that the ambient currents were much weaker in Donelan et al.'s area of observations in Lake Ontario, with negligible tides, than those in the JONSWAP area of observations in the German Bight, with significant tides.

The mean values of β from this study are compared in Table 2 with values reported in the literature. All entries in this table, except those of the present study and those referring to Donelan et al. (1985), have been obtained from Phillips (1985). Reference is made to appendix B for our estimation of a mean β value from the data of Donelan et al.

A striking outlier in Table 2 is the value of β from the laboratory data of Toba (1973). It is much lower than those obtained from the field data. Phillips (1985) ascribes this difference to strong wind-drift effects in the laboratory experiments.

The values of β obtained from previous field data vary from 0.06 to 0.11. As pointed out by Phillips (1985) there appears to be a remarkable geographically based dichotomy in these results, the Pacific data being considerably lower than the non-Pacific data. The mean value of β from the present study, based on the JONSWAP observations (0.13, with a standard deviation of about 0.06) is somewhat higher than those from the other non-Pacific field data. This difference is

somewhat larger than the estimated bias of 10% due to the tidal currents during the JONSWAP observations (section 46).

7. Conclusions

A reanalysis of the original spectra measured in the JONSWAP campaign indicates that the high-frequency part of the wave spectrum can be better approximated with an f^{-4} tail than with an f^{-5} tail. The difference in goodness-of-fit is statistically significant at a level of confidence of 99.9%.

The estimated values of the energy scale parameter β in the Toba spectrum are found to be virtually independent of the stage of wave development represented by the dimensionless peak frequency ν. This finding is consistent with Toba's hypothesis that β should be a universal constant. However, it differs from the data of Donelan et al. (1985), whose results indicate a noticeable increase of β with a decrease in ν.

The β values as determined from the JONSWAP data display a relatively large scatter and their average value is slightly higher than the mean values reported in the literature. This large scatter and the difference

APPENDIX A

Spectral Characteristics

In the following table the characteristics are given of the 99 observed spectra used in the present study. These data, including the serial numbers, are copied from Müller (1976). The spectra marked with * are not used in the high-frequency range analysis.

Serial number	f_m (Hz)	U_{10} (m s^{-1})	Serial number	f_m (Hz)	U_{10} (m s^{-1})	Serial number	f_m (Hz)	U_{10} (m s^{-1})
*14	0.538	7.8	49	0.361	10.7	84	0.351	12.7
15	0.276	7.8	50	0.338	10.7	85	0.455	12.7
16	0.305	7.8	51	0.384	10.0	*86	0.595	11.8
17	0.380	7.8	52	0.280	10.0	87	0.491	11.8
18	0.382	8.8	53	0.400	10.0	89	0.409	9.7
19	0.322	8.8	54	0.299	9.7	*90	0.504	9.7
20	0.387	8.8	55	0.391	9.7	91	0.465	8.0
*21	0.617	8.8	56	0.407	8.3	92	0.405	8.5
22	0.344	8.8	57	0.350	8.8	93	0.419	8.5
23	0.457	7.7	58	0.429	8.8	*94	0.512	9.8
25	0.465	8.0	*59	0.581	8.8	95	0.398	9.8
26	0.317	8.0	60	0.283	10.3	96	0.337	9.8
27	0.418	8.0	61	0.451	11.8	97	0.369	9.8
28	0.283	8.7	62	0.346	11.8	98	0.326	12.7
29	0.294	8.7	63	0.374	11.8	99	0.298	12.7
30	0.369	8.7	64	0.266	11.8	*100	0.570	12.3
31	0.302	9.0	65	0.251	12.3	101	0.423	12.3
32	0.452	9.0	66	0.237	12.3	102	0.462	8.2
33	0.405	8.7	67	0.295	12.3	103	0.382	8.2
*34	0.569	8.7	*68	0.581	12.0	104	0.355	9.7
35	0.459	8.7	69	0.451	12.0	105	0.445	9.7
*36	0.647	8.7	70	0.401	10.7	106	0.401	11.7
37	0.375	9.0	71	0.263	10.7	*107	0.512	11.7
*38	0.599	9.0	72	0.456	8.7	108	0.360	11.7
39	0.338	9.0	73	0.269	8.7	111	0.466	9.5
*40	0.649	9.3	*74	0.593	8.7	112	0.349	9.3
41	0.393	9.3	77	0.379	10.3	113	0.422	6.2
42	0.358	9.7	78	0.432	10.3	*114	0.512	12.7
43	0.328	9.7	*79	0.590	10.3	117	0.320	6.3
*44	0.608	9.7	80	0.461	9.7	118	0.320	6.2
46	0.269	10.7	81	0.397	9.7	119	0.325	6.2
47	0.278	10.7	82	0.340	12.0	120	0.395	5.6
48	0.425	10.7	83	0.350	12.0	121	0.468	5.6

in mean value can in part be ascribed to the influence of tidal currents.

Acknowledgments. We greatly appreciate the permission of the JONSWAP group to use their original data for a reanalysis. In addition we thank T. I. Bern, now at the Oceanographic Company of Norway, for assisting us in implementing the simplex minimization method.

APPENDIX B

Transformation of Results of Donelan et al. (1985)

The expression for the high-frequency spectrum given by Donelan et al. (1985) can be written as

$$E(\omega) = \alpha_D g^2 \omega_m^{-1} \omega^{-4}. \quad \text{(B1)}$$

Comparison with Toba's formulation (3) shows that

$$\beta = \left(\frac{\omega_m u_*}{g}\right)^{-1} \alpha_D \quad \text{(B2)}$$

which can be expressed in terms of $\nu = f_m U_{10}/g$ as

$$\beta = (2\pi)^{-1} c_d^{-1/2} \nu^{-1} \alpha_D \quad \text{(B3)}$$

using $c_d = (u_*/U_{10})^{1/2}$. This transformation has been applied to the α_D values given in Fig. 13 of Donelan et al. The result is shown in Fig. 5, where $c_d = 1.5 \times \times 10^{-3}$ has been used. The corresponding mean value of β is estimated as $\bar{\beta} \approx 0.11$.

Donelan et al. give the following parameterization of α_D:

$$\alpha_D = 0.006\, \tilde{\omega}_m^{0.55} \quad \text{for} \quad 0.83 < \tilde{\omega}_m < 5 \quad \text{(B4)}$$

in which $\tilde{\omega}_m = \omega_m U_{10} \cos\theta/g$, and $U_{10} \cos\theta$ is the component of the wind velocity at 10 m elevation in the direction of wave propagation at the spectral peak. With the approximation $\cos\theta \approx 1$, we have $\tilde{\omega}_m \approx 2\pi\nu$, in which case substitution of (B4) into (B3) gives

$$\beta = 0.006(2\pi)^{-0.45} c_d^{-0.5} \nu^{-0.45} \cong 0.068\, \nu^{-0.45}. \quad \text{(B5)}$$

REFERENCES

Donelan, M. A., J. Hamilton and W. H. Hui, 1985: Directional spectra of wind-generated waves. *Phil. Trans. Roy. Soc. London,* **A315,** 509–562.

Draper, N. R., and H. Smith, 1981: *Applied Regression Analysis,* 2nd ed., Wiley.

Forristall, G. Z., 1981: Measurements of a saturated range in ocean wave spectra. *J. Geophys. Res.,* **86**(C9), 8075–8084.

Garrett, J. R., 1977: Review of drag coefficients over oceans and continents. *Mon. Wea. Rev.,* **105,** 915–929.

Hasselmann, K., T. P. Barnett, E. Bouws, H. Carlsen, D. E. Cartwright, K. Enke, J. A. Ewing, H. Gienapp, D. E. Hasselmann, P. Kruseman, A. Meerburg, P. Müller, D. J. Olbers, K. Richter, W. Sell and H. Walden, 1973: Measurements of wind-wave growth and swell decay during the Joint North Sea Wave Project (JONSWAP). *Dtsch. Hydrogr. Z.,* **A8**(12).

——, D. B. Ross, P. Müller and W. Sell, 1976: A parametric wave prediction model. *J. Phys. Oceanogr.,* **6,** 200–228.

Kahma, K. K., 1981: A study of the growth of the wave spectrum with fetch. *J. Phys. Oceanogr.,* **11,** 1503–1515.

Kawai, S., K. Okada and Y. Toba, 1977: Field data support of three-seconds power law and $gu_*\sigma^{-4}$ spectral form for growing wind waves. *J. Oceanogr. Soc. Japan,* **33,** 137–150.

Kitaigorodskii, S. A., 1983: On the theory of the equilibrium range in the spectrum of wind-generated gravity waves. *J. Phys. Oceanogr.,* **13,** 816–827.

——, V. P. Krasitskii and M. M. Zaslavskii, 1975: On Phillips' theory of equilibrium range in spectra of wind-generated gravity waves. *J. Phys. Oceanogr.,* **5,** 410–420.

Kondo, J., Y. Fujinawa and G. Naito, 1973: High-frequency components of ocean waves and their relation to the aerodynamic roughness. *J. Phys. Oceanogr.,* **3,** 197–202.

Mitsuyasu, H., F. Tasai, T. Suhara, S. Mizuno, M. Ohkusu, T. Honda and K. Rikiishi, 1980: Observations of the power spectrum of waves using a cloverleaf buoy. *J. Phys. Oceanogr.,* **10,** 286–296.

Müller, P., 1976: Parameterization of one-dimensional wind wave spectra and their dependence on the state of development. *Hamburger Geophys. Einzelschriften,* **31,** Hamburg University.

Nelder, J. A., and R. Mead, 1965: A simplex method for function minimization. *Comput. J.,* **7,** 308–313.

Phillips, O. M., 1958: The equilibrium range in the spectra of wind-generated waves. *J. Fluid Mech.,* **4,** 426–434.

——, 1985: Spectral and statistical properties of the equilibrium range in wind-generated gravity waves. *J. Fluid Mech.,* **156,** 505–531.

Pierson, W. J., and L. Moskowitz, 1964: A proposed spectral form for fully developed wind seas based on the similarity theory of S. A. Kitaigorodskii. *J. Geophys. Res.,* **69**(24), 5181–5190.

Toba, Y., 1972: Local balance in the air–sea boundary processes. I: On the growth process of wind waves. *J. Oceanogr. Soc. Japan,* **28,** 109–121.

——, 1973: Local balance in the air–sea boundary process. III: On the spectrum of wind waves. *J. Oceanogr. Soc. Japan,* **29,** 209–220.